WINFIELD H. FARTHING

THE MAGSAT SCALAR MAGNETOMETER

The Magsat scalar magnetometer is derived from optical pumping magnetometers flown on the Orbiting Geophysical Observatories. The basic sensor, a cross-coupled arrangement of absorption cells, photodiodes, and amplifiers, oscillates at the Larmor frequency of atomic moments precessing about the ambient field direction. The Larmor frequency output is accumulated digitally and stored for transfer to the spacecraft telemetry stream. In orbit the instrument has met its principal objective of calibrating the vector magnetometer and providing scalar field data.

INTRODUCTION

The cesium vapor optical pumping magnetometer used on Magsat is derived from the rubidium magnetometers flown on the Orbiting Geophysical Observatories (OGO) between 1964 and 1971. The Polar Orbiting Geophysical Observatories (Pogo) used rubidium-85 optical pumping magnetometers,[1] while those on the Eccentric Orbiting Geophysical Observatories (Eogo) used the slightly higher gyromagnetic ratio of rubidium-87.

Data generated by the Pogo instruments provided the principal data base for the U.S. input to the World Magnetic Survey,[2] an international cooperative effort to survey and model the geomagnetic field. It is partly this body of data that underlies the most accurate analytical models of the main geomagnetic field in present use.[3] Further studies of the Pogo data base and other sources led to the recognition of the need for a dedicated mission, such as Magsat, to increase the resolution for crustal studies, to incorporate vector measurements, and to correct the models for secular variation.

When considering various options for implementing a scalar magnetometer for use in space, optical pumping instruments are clearly superior in view of requirements for accuracy, dynamic range, information bandwidth, ease of data collection and storage, power and weight requirements, and reliability. For the self-oscillating type used in OGO and Magsat, cesium-133 is superior to other alkali vapors because of its narrower resonance line width, followed by rubidium-87 and rubidium-85. When instrumentation for Pogo was selected, cesium had not been used extensively in magnetometry and thus was not considered sufficiently developed to use in spaceflight. Rubidium-87, with its higher gyromagnetic ratio, would have resulted in a wide range of frequencies over which it would have been difficult to control the electronic phase shifts that are so important to accuracy. Rubidium-85, with its gyromagnetic ratio of 4.66737 Hz per nanotesla (nT), was therefore used even though, from the standpoint of resonance line width, it is the poorest of the three. In the interim between OGO and Magsat, cesium-133 came to be the most commonly used isotope in alkali vapor magnetometry and was thus the natural selection for Magsat.

PRINCIPLE OF SENSOR OPERATION

The alkali vapor magnetometer is based on the phenomenon of optical pumping reported by Dehmelt[4] in 1957. The development of practical magnetometers followed rapidly, evolving in one form finally to the dual-cell, self-oscillating magnetometer[5] shown in Fig. 1. Two of these twin-cell magnetometers are combined in the Magsat magnetometer. In each twin-cell sensor an electrodeless discharge lamp driven by the RF exciter produces resonance radiation that is collimated and passed through an interference filter, which selects the D_1 spectral line (894.5 nm for cesium-133) and rejects the D_2 spectral line (852.1 nm for cesium-133). The light is then circularly polarized before it is allowed to optically excite cesium vapor contained in the absorption cells.

Two identical sets of optics are employed, with the direction of light propagation antiparallel, thus defining the "optical axis" of the system. The transmission of each absorption cell is monitored by a photodetector, amplified, and cross-fed back to solenoidal coils wound about the absorption cells coaxially with the optical axis. A closed loop is thus formed that oscillates if the loop gain is greater than unity at the frequency where the loop phase shift is zero. The frequency of oscillation is a direct measure of the strength of the ambient magnetic field, i.e., the Larmor frequency of atomic magnetic moments precessing about the ambient field direction.

The modulation of light transmission obtained through application of a Larmor frequency signal to the solenoidal coil, termed the "H_1" coil, results from transitions between the discrete hyperfine

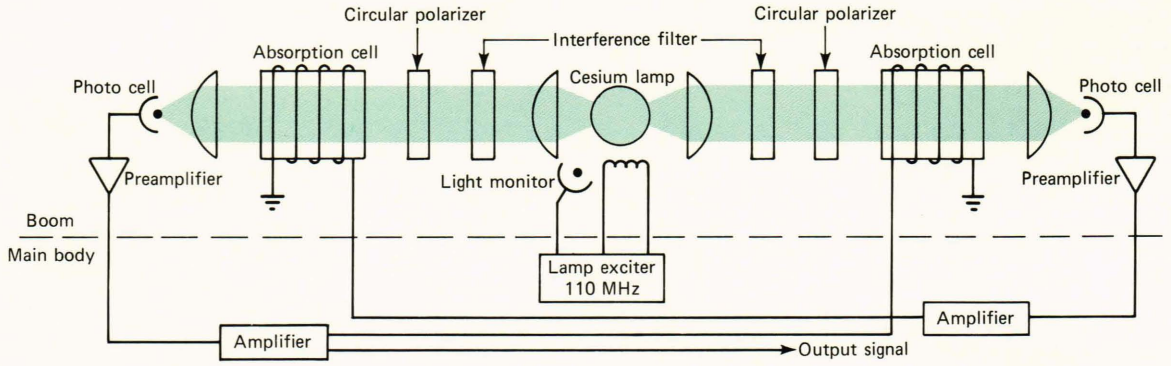

Fig. 1—Dual-cell cesium magnetometer. The loop, composed of absorption cells, photocells, and amplifiers oscillates at a frequency proportional to the ambient field magnitude.

energy states that exist in the cesium atom when it is subjected to a magnetic field. The hyperfine splitting of cesium-133 is shown in Fig. 2. Prior to the application of pumping light, the atoms can be considered to have a Boltzmann distribution among the energy states. Optical pumping polarizes the sample so that a nonequilibrium concentration of atoms in either the m (the Larmor frequency for transition) $= +4$ or $m = -4$ sublevel of the ground state is obtained, depending on both the sense of circular polarization and the direction of the optical axis component of the magnetic field.

Application of a (Larmor frequency) signal to the H_1 coil at the transition frequency for $m = +4, +3$ (or $m = -4, -3$) causes the selective depumping of a group of atoms having a certain phase with the driving signal. Since the pumping probability depends on the angle to the light wave normal as the group of depumped atoms precesses, the light transmission is modulated at the Larmor frequency.

A single-cell absorption cell process is subject to "heading error" in that the Larmor frequency for transition $m = +4, +3$ differs from that for transition $m = -4, -3$. The dual-gas-cell configuration has a strong advantage over single-cell magnetometers in that the sense of circular polarization is such that when one cell is pumped to the $m = +4$ state, the other is pumped to the $m = -4$ state, resulting in a reverse skew for the two absorption cells. Since the dual-cell loop transfer function includes the product of the individual absorption lines, a symmetrical two-cell composite line is obtained. Thus the frequency of operation should not change under reversal of the ambient field with respect to the sensor.

The frequency of oscillation of the loop is determined by the open loop phase shift of all the components. If the net phase shift from all sources other than the absorption cells is zero at any frequency, the closed loop oscillates at the frequency where the phase shifts of the two absorption cells are equal and opposite. By the symmetry of the system, this frequency is the average of the eight

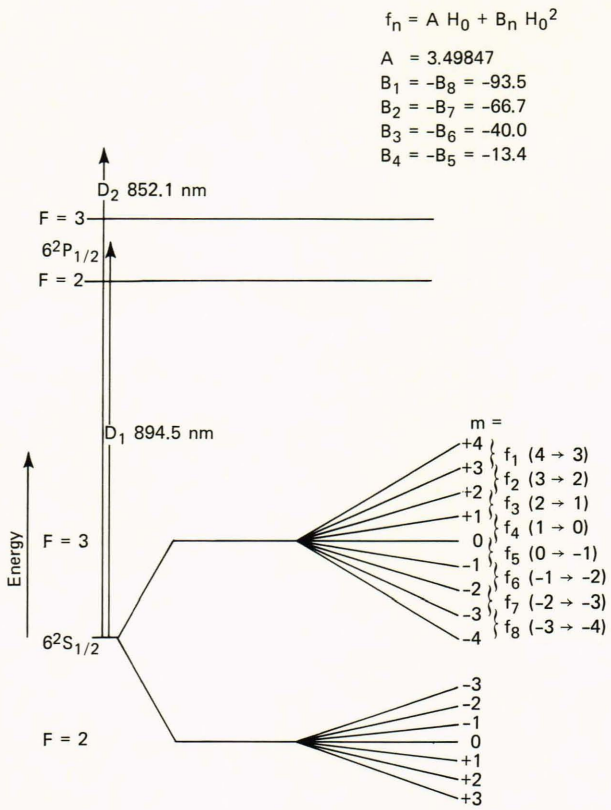

Fig. 2—Energy diagram for cesium-133. Transition frequencies f_1 to f_8 are in hertz for the applied field H_0 in gauss (1 gauss = 10^5 nT).

absorption frequencies of the Zeeman spectrum for $F = 3$. This yields for the theoretical oscillation frequency

$$f = 3.49847\, H_0 ,$$

where f is given in hertz if the ambient field H_0 is expressed in nanoteslas.

The various processes of modulating and monitoring light in the twin-cell sensor are such that the loop gain depends on the product $\sin^2 \theta \cos \theta$, where θ is the angle between the optical axis and

the applied field. Thus null zones are to be expected in a twin-cell sensor when the ambient field is either along or perpendicular to the optical axis. These zones are termed "polar" and "equatorial" null zones, respectively. The Magsat magnetometer incorporates two such sensors, with their optical axes crossed at 55°. The polar null zones are thereby eliminated because they have no intersection, and the only remaining composite null zone is the intersection of the two equatorial null zones, shown in Fig. 3. In the Magsat magnetometer, the composite null zone is directed normal to the orbit plane, such that in normal operation in near-polar orbit the ambient field will never lie within the composite null zone.

It is desired, of course, to minimize the width of the null zones for each individual sensor. It is thus necessary to use high gain amplifiers in the system, the limitations being the noise level of the system and the requirement to maintain near-zero phase shift over the operating frequency range. The width of the null zones is also quite dependent on the operating temperature of the absorption cells. For cesium-133, the optimum cell temperature is 52°C. The four absorption cells in the Magsat magnetometer are maintained at the desired temperature by individual thermostatically controlled heaters. The heaters are made from bifilar-wound resistance wire to avoid magnetic signature, and each heater dissipates 0.5 W at 30 V when the thermistor-operated control circuitry closes the circuit. The overall thermal environment is achieved by controlling separately the beryllia yoke (into which the sensors are mounted) at 41°C, and enclosing the entire sensor in a passive thermal enclosure with a radiator whose area is selected to radiate the required amount of energy. Figure 4 shows the Magsat scalar magnetometer sensor configuration without its thermal enclosure or radiator.

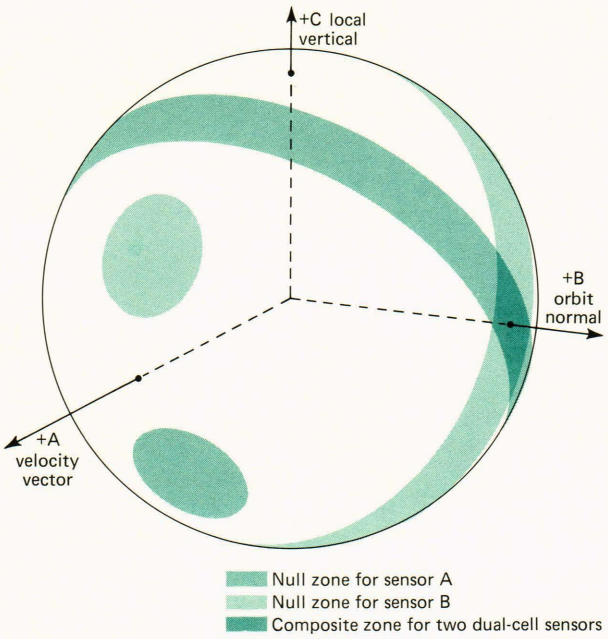

Fig. 3—Spatial coverage of the scalar magnetometer. The composite null zone, or intersection of the two individual sensor null zones, is oriented normal to the spacecraft orbit plane. It should never contain the magnetic field vector.

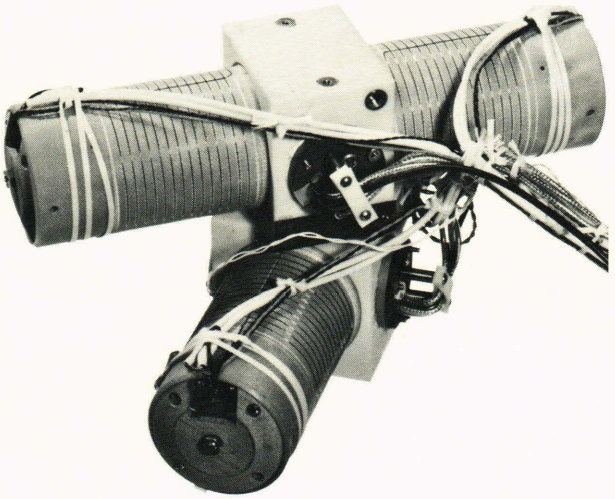

Fig. 4—Magsat scalar magnetometer sensor. Each cylinder contains optics and hybrid preamplifiers for one dual cell magnetometer. The central yoke is made of beryllia to minimize the temperature gradient. A flat beryllia radiator (not shown) is attached to the top of the yoke. The entire structure is housed in a fiberglass and multilayer thermal blanket enclosure.

DIGITAL DATA GENERATION

Figure 5 is a diagram of the electronics necessary to operate the sensors and to interface the spacecraft telemetry system. In order to prevent interference between the two sensors, they must be operated in frequency lock. This is accomplished by using a combining amplifier on one side of the sensors. The combining amplifier is repeated in order to implement fully the design objective of maintaining the maximum amount of redundancy for single sensor operation. The output signals from the two combining amplifiers are processed through completely independent signal processors consisting of phase-locked loop tracking filters, accumulators, and readout gates. In each signal processor chain, the bandwidth of the tracking filter is set at 25 Hz to ensure that the loop will track the varying input frequency adequately and to make negligible any errors associated with time lag in the closed-loop transfer function. The accumulators are of a commandable aperture type, a design feature that was incorporated to allow the sampled data to vary from the normal situation of a 30 ms aperture time (in which the information bandwidth is primarily that of the tracking filter) to a maximum aperture case (where the frequency characteristic of the sampling function is primarily determined by the aperture time and the resulting output data are substantially protected from frequency aliasing effects). In

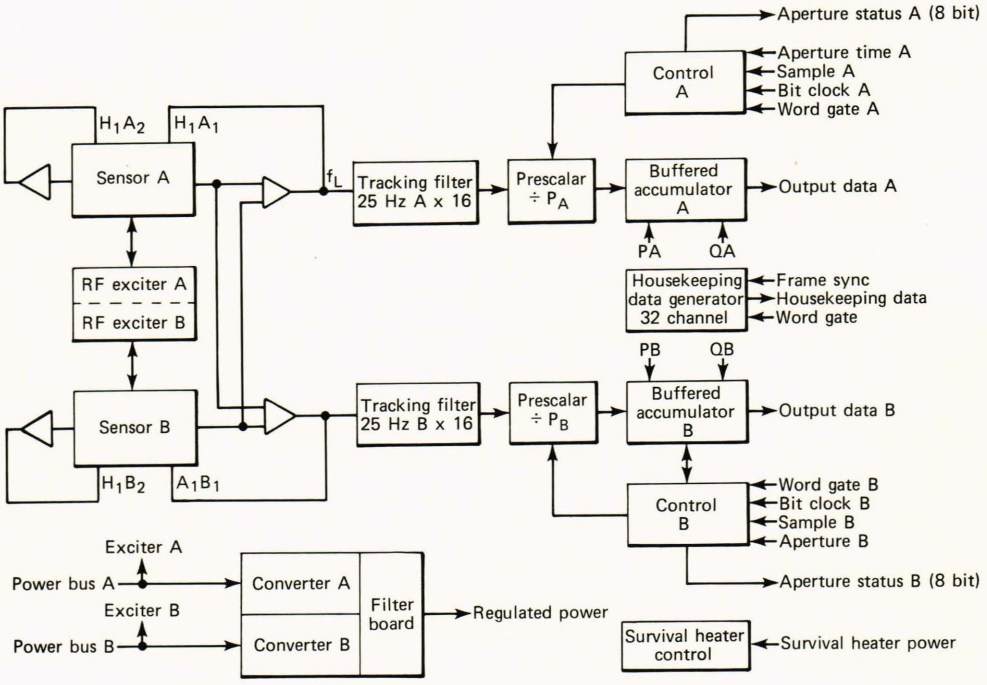

Fig. 5—Block diagram of scalar magnetometer electronics.

order to make this design objective compatible with resolution requirements, the tracking filters were designed to multiply the Larmor frequency by a factor of 16.

The output data word assigned to each scalar magnetometer data point is 20 bits long. The last bit is made a parity bit, and the next to last bit was desired to be a data quality flag associated with that particular sample. This leaves 18 bits for the primary data sample, which was not compatible with the full range of commandable aperture times. Thus a prescalar is included in each data processing chain. The prescalar is under the control of the commanded aperture time, which is delivered to the experiment in the form of a binary number, N, that specifies the aperture time as $(2N + 1)Tb$, where Tb is the telemetry bit time of 0.512 ms. For $N \leq 63$, the prescalar factor, P, is 1. For $64 \leq N \leq 127$, the prescalar factor is 2. For $N \geq 128$, the prescalar factor divides by 4.

The logic equation for the data quality flag, Q, associated with each data point is, for instance, for scalar A,

$$Q_A = T_{FA} \cdot (\mathrm{SIGA} + \mathrm{SIGB}) \cdot (\mathrm{BRA} + \mathrm{BRB}) ,$$

where each term in the logic function has to be true over the accumulation time in which that particular data sample was collected. $T_{FA} = 1$ means that the tracking filter associated with that data point was in lock throughout the accumulation time. SIGA + SIGB = 1 is a condition that the signal amplitude in either sensor A or sensor B is above a predetermined threshold throughout the accumulation interval. BRA + BRB = 1 is a condition that one or both of the lamps must be operating within a predetermined brightness range throughout the accumulation interval. This form of the logic function was selected in order to be compatible with the operation of both processing chains with a single sensor and yet to be an efficient rejector of a number of possible malfunctions within the instrument.

The sampling of each scalar is done at 4 samples per second, and the samples of scalar A and scalar B are interleaved to obtain a total of 8 equidistant samples per second.

OPERATION IN ORBIT

The Magsat scalar magnetometer met its principal in-orbit objective of calibrating the vector magnetometer and returned scalar field data, although intermittent noise in the lamp excitation circuitry caused loss of lock in the tracking filters and, therefore, a reduction in the expected data rate.

Engineering data returned from the instrument verified that the thermal control circuitry performed as expected in controlling lamp and absorption cell temperatures. Monitors in the lamp RF control loops were only reliable when the intermittent noise was absent but at such times showed that lamp A operated at control parameters identical to those observed during ground thermal-vacuum testing. Lamp B, which ran extremely efficiently during ground testing, required slightly more RF power in orbit. Sensors A and B were operated independently at times to serve as a cross check on absolute accuracy and to verify the integrity of the Larmor sensors.

The lamp noise problem manifested itself differently in the two lamps. It first appeared in lamp A about 12 hours after the instrument was turned on and, except for a few periods after the lamp had been off for a day or more, was consistently present in the lamp excitation until the spacecraft entered the eclipse season, when a dramatic improvement occurred. The problem was first observed in lamp B two weeks after turn-on and was present intermittently over a period of several hours in a way that has not been explained. Transitions from one state to another often occurred when one of the tape recorders was played back, but the problem was not associated with a particular tape recorder. The lamp problem was most likely caused by a feedback mechanism to the spacecraft power that was not present to the same degree on the ground.

The effect of the interference on tracking filter lock was much more serious when the noise was present in lamp B. Thus the operational mode was to operate lamp A continuously and to operate lamp B approximately one day out of five in order to fill in the A sensor null zones and to provide a more complete data set for calibration of the vector magnetometer.

Incorporation of the data quality flag in the output word proved indispensable to the rejection of data when the tracking filter was out of lock and enabled the combination of vector and scalar magnetometers to meet substantially all the objectives, even in the presence of the lamp excitation noise.

REFERENCES

[1]W. H. Farthing and W. C. Folz, "Rubidium Vapor Magnetometer for Near Earth Orbiting Spacecraft," *Rev. Sci. Instrum.* **38**, pp. 1023 – 1030 (1967).

[2]A. J. Zmuda (ed.), *The World Magnetic Survey*, IAGA Bulletin No. 28 (1971).

[3]Ibid., p. 148.

[4]H. G. Dehmelt, *Phys. Rev.* **105**, p. 1487 (1957).

[5]A. L. Bloom, "Principles of Operation of the Rubidium Vapor Magnetometer," *Appl. Opt.* **1**, pp. 61 – 68 (1962).

ACKNOWLEDGMENT — The Magsat scalar magnetometer was built for the NASA/Goddard Space Flight Center by Bell Aerospace Systems Division, Western Laboratories, and Varian Associates, Canada, Ltd. Mr. David Synder, BASD, was program manager for the project. The RF exciters were provided by Mr. L. J. Rogers of GSFC.